Explainable Machine Learning for Mechanistic Analysis of Irradiation-Induced Tensile Behavior in Fast Reactor Cladding

Hongin Kim[a, b], Sunghwan Yeo[a] , Jun-Hwan Kim[a], Jeong Mok Oh[a,*] Young-Kook Lee[b]
[a]*Advanced Fuel Technology Development Division, Korea Atomic Energy Research Institute, Daedeok-daero 989-111, Yuseong-gu, Daejeon, 34057, Republic of Korea*
[b]*Department of Materials Science and Engineering, Yonsei University, Seoul, 03722, Republic of Korea*
[*]*Corresponding author: jeongmokoh@kaeri.re.kr*

Keywords : Tensile properties, Neutron irradiation, Ferritic/Martensitic Steels (FMS), Nuclear fuel cladding, Machine learning

1. Introduction

Generation IV reactors are being developed to achieve enhanced safety and economic competitiveness compared with Generation III/III+ reactors [1]. As high-temperature and high-burnup operation is considered, nuclear fuel cladding is exposed to harsh service environments, including long-term high-temperature exposure and neutron irradiation [2]. As the neutron irradiation dose (displacements per atom, dpa) increases, cladding materials undergo irradiation-induced degradation [3, 4]. In this context, 9–12Cr ferritic/martensitic (F/M) steels such as HT9 and Gr.92 are regarded as important comparative cladding candidates for evaluating applicability in reactor environments [5].

Reliable characterization and prediction of irradiation effects require systematic acquisition of tensile property data over a wide range of irradiation dose and temperature combinations. However, neutron irradiation testing and post-irradiation examination (PIE) are time- and cost-intensive. Inaddition, they are constrained by the limited availability of research reactors capable of neutron irradiation and by hot-cell testing facilities [6].

Empirical models, such as dispersed barrier hardening (DBH) and saturation-type relations, have been used to interpret irradiation-induced property changes [7, 8]. However, tensile property evolution is a multidimensional outcome governed by coupled effects of alloy composition, heat treatment, and irradiation conditions; thus, simplified relations alone are insufficient to consistently describe trends across diverse materials and conditions. Accordingly, a machine-learning (ML) approach provides a practical route to predict tensile properties under multidimensional irradiation conditions and to identify the primary governing factors [9]. In addition, applying explainable artificial intelligence (XAI) enables quantitative evaluation of feature contributions [10].

In this study, we develop ML models to predict the tensile properties of HT9 and Gr.92 (Mod) under neutron irradiation conditions and use XAI to analyze their sensitivity to irradiation damage and temperature effects, and to quantify key factor contributions.

2. Experimental procedure

2.1 ML dataset

In this study, a total of 1,569 tensile data points were collected from public literature and reports, and the basic statistics of the collected data are summarized in Table 1. The 9–12Cr FMS dataset includes alloy chemistry, heat treatment, irradiation and test conditions, and tensile properties. The ML models used 26 input variables, and the output variables were three tensile propertiesultimate tensile strength (UTS), yield strength (YS), and elongation (El). The dataset was randomly split into training (64%), validation (16%), and test (20%) sets, and model performance was evaluated on the test set using RMSE and R^2.

2.2 Regression ML modeling

Five regression algorithms were employed, including Elastic Net (EN), Support Vector Regression (SVR), Random Forest (RF), eXtreme Gradient Boosting (XGB), and an Artificial Neural Network (ANN) [11–15]. Hyperparameters were optimized using Optuna with 1,000 trials per model, where the objective function minimized the mean validation RMSE across the three standardized outputs [16]. In addition, to reduce split-dependent variation, the final performance was further evaluated using repeated 10-fold cross-validation (three repeats, 30 evaluations total). All pipelines were implemented in Python 3.11.

2.3 Explainable Artificial Intelligence (XAI)

To enhance interpretability, XAI methods were applied to quantify the extent to which input variables contributed to the predictions. In this study, Shapley Additive exPlanations (SHAP) was adopted as the primary method because it can evaluate both the direction and magnitude of feature contributions at the sample level [17]. To reduce computational cost, SHAP values were estimated using dropout- and gradient-based approximation methods. To clearly isolate irradiation effects, a non-irradiated baseline was defined, and relative contributions under neutron-irradiation conditions were evaluated against this baseline.

2.4 Experimental validation

Independent tensile datasets for HT9 and Gr.92 (Mod) were obtained for validation and were not included in model training. Heat treatment for HT9 and Gr.92 steels consisted of normalizing at 1050 ℃ for 30 min and tempering at 750 ℃ for 60 min, followed by air cooling. Tensile specimens were machined into miniature dog-bone geometries with a gauge section of 7.62 × 1.52 × 0.79 mm, and the strain rate was set to 1×10^{-3} s^{-1}. Neutron irradiation was conducted in the BOR-60 reactor at an irradiation temperature of 600 ℃ with doses up to 33 dpa.

Table 1. Data used for machine learning modeling of mechanical properties damaged by neutron irradiation.

Variables	Data range	Mean ± s.d.
C (wt%)	0.05–0.23	0.12 ± 0.04
Si (wt%)	0–1.11	0.24 ± 0.19
Mn (wt%)	0–1.08	0.45 ± 0.14
Ni (wt%)	0–2.27	0.28 ± 0.47
Cr (wt%)	7.52–12.90	9.48 ± 1.43
Mo (wt%)	0–2.31	0.60 ± 0.49
W (wt%)	0–3.08	0.83 ± 0.87
Cu (wt%)	0–1.02	0.06 ± 0.18
B (wt%)	0–0.09	0.01 ± 0.02
Al (wt%)	0–0.04	0.01 ± 0.01
N (wt%)	0–0.30	0.03 ± 0.03
Ti (wt%)	0–0.06	0.01 ± 0.01
V (wt%)	0–0.35	0.20 ± 0.07
Nb (wt%)	0–0.40	0.04 ± 0.04
Co (wt%)	0–0.15	0.01 ± 0.02
Ta (wt%)	0–1.60	0.03 ± 0.10
Normalizing (℃)	880–1150	1033.8 ± 34.2
Normalizing time (min)	10–120	44.0 ± 19.6
Tempering (℃)	620–820	744.6 ± 42.1
Tempering time (min)	30–422	109.6 ± 87.4
Test temp (℃)	25–760	327.4 ± 223.0
Strain rate ($\times 10^{-4}$ /s)	0.01–2670	52.5 ± 273.6
Aging (℃)	28–704	150.4± 232.4
Aging time (h)	0–100000	4710.8 ± 13674.9
Dose (dpa)	0–77.9	4.9 ± 12.2
Irradiation temp (℃)	25–802	116.0 ± 159.1
Tensile strength (MPa)	97–1468	635.3 ± 238.9
Yield strength (MPa)	73–1451	549.5 ± 239.3
Elongation (%)	0.12–77	18.3 ± 11.7

3. Results and Discussion

In ML modeling, not only predictive accuracy but also generalization performance to prevent overfitting is important. Table 2 presents the objective-function RMSE of each ML model and the k-fold cross-validation results of R^2 for each output. The tree-based models, RF and XGB, showed strong predictive and generalization performance. However, because these models rely on rule-based splitting, they may have limitations in representing continuous nonlinear trends. Therefore, this study selected the ANN as the final model. The ANN achieved the second-lowest RMSE and R^2 values above 0.9, indicating robust performance.

Table 2. Objective values and K-fold cross-validation results for each regression model.

Model	Objective value (RMSE)	K-fold CV (R^2)		
		UTS	YS	El
EN	0.37	0.86	0.84	0.81
RF	0.29	0.95	0.94	0.91
XGB	0.24	0.96	0.95	0.92
SVM	0.31	0.93	0.92	0.88
ANN	0.27	0.94	0.93	0.91

Fig. 1 compares the ANN predictions with experimental tensile properties of HT9 and Gr.92 under unirradiated and irradiated conditions. The experimental data used for comparison were independent data not included in model training, confirming that the ANN provides sufficient predictive accuracy for both alloys. The model also captured the nonlinear behavior associated with dynamic strain aging in the temperature range of approximately 250–450 ℃.

In addition, the tensile properties measured after neutron irradiation at 600 ℃ were in good overall agreement with the ANN predictions (red-boxed region, unpublished data). Meanwhile, no clear irradiation hardening was observed over the irradiated data range analyzed in this study (12–33 dpa). This behavior is attributed to the combined effects of relatively low neutron flux depending on in-core position and long-term high-temperature exposure, which together promote microstructural degradation and defect recovery, thereby offsetting the strengthening effect.

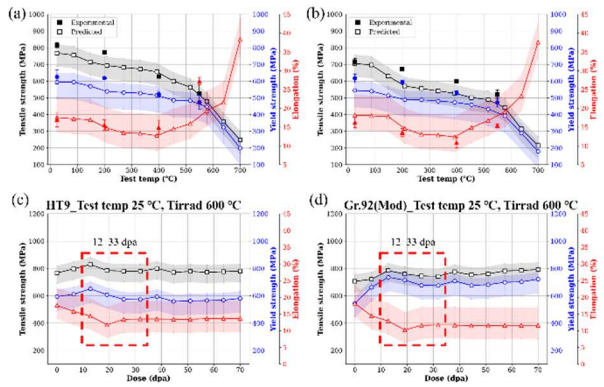

Fig. 1. Comparison between experiments and ANN predictions. (a, b) unirradiated HT9 and Gr.92 and (c, d) neutron irradiated specimens at room temperature.

Fig. 2 shows the SHAP analysis results for the ML dataset. The features were ranked in order of contribution, and the color of each data point represents the feature magnitude, with higher values indicated in red. For yield strength, the dominant factors were test temperature, dpa, and irradiation temperature. Temperature is considered to affect yield strength by influencing deformation and fracture mechanisms and by driving microstructural changes such as recovery and precipitation behavior. In addition, increasing dpa contributes to higher yield strength by promoting the development of dislocation

structures and the accumulation of point defects, including vacancies and defect clusters, which impede dislocation motion.

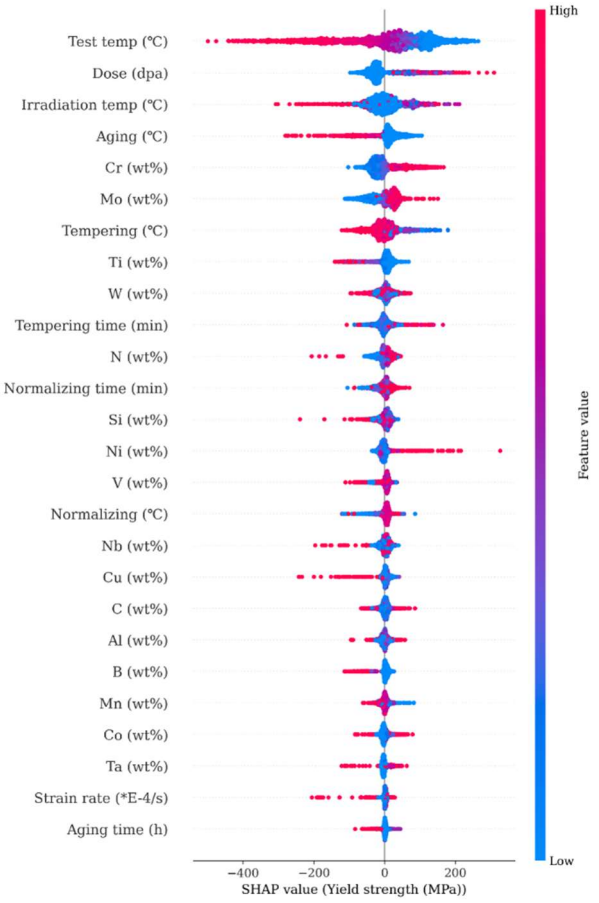

Fig. 2. SHAP summary (beeswarm) plots for yield strength (MPa).

4. Conclusion

This study developed a machine learning model to predict the tensile properties of FM steels. Model performance and interpretability were also evaluated. The optimized ANN provided high predictive accuracy and reasonably reproduced the temperature-dependent and nonlinear behavior observed in independent experimental data. SHAP analysis identified test temperature, dpa, and irradiation temperature as the dominant factors. These results indicate that irradiation damage and temperature-driven microstructural evolution govern tensile property changes. Machine learning can not only predict mechanical property changes under neutron irradiation effectively but also provide interpretable insights by separating the key factors through XAI. Future work will focus on quantifying the contribution of each factor and evaluating alloy-specific sensitivities to these factors.

REFERENCES

[1] J.E. Kelly, Generation IV International Forum: A decade of progress through international cooperation, Progress in Nuclear Energy 77 (2014) 240-246.
[2] S.J. Zinkle, G.S. Was, Materials challenges in nuclear energy, Acta Materialia 61(3) (2013) 735-758.
[3] Y. Chen, IRRADIATION EFFECTS OF HT-9 MARTENSITIC STEEL, Nuclear Engineering and Technology 45(3) (2013) 311-322.
[4] F.A. Garner, M.B. Toloczko, B.H. Sencer, Comparison of swelling and irradiation creep behavior of fcc-austenitic and bcc-ferritic/martensitic alloys at high neutron exposure, Journal of Nuclear Materials 276(1) (2000) 123-142.
[5] R.L. Klueh, Analysis of swelling behaviour of ferritic/martensitic steels, Philosophical Magazine 98(28) (2018) 2618-2636.
[6] P. Wang, Q. Tao, H. Dong, G.M.A.M. El-Fallah, Advanced machine learning analysis of radiation hardening in reduced-activation ferritic/martensitic steels, Computational Materials Science 251 (2025) 113773.
[7] L. Tan, J.T. Busby, Formulating the strength factor α for improved predictability of radiation hardening, Journal of Nuclear Materials 465 (2015) 724-730.
[8] A.D. Whapham, M.J. Makin, The hardening of lithium fluoride by electron irradiation, The Philosophical Magazine: A Journal of Theoretical Experimental and Applied Physics 5(51) (1960) 237-250.
[9] I.D. Jung, D.S. Shin, D. Kim, J. Lee, M.S. Lee, H.J. Son, N.S. Reddy, M. Kim, S.K. Moon, K.T. Kim, J.-H. Yu, S. Kim, S.J. Park, H. Sung, Artificial intelligence for the prediction of tensile properties by using microstructural parameters in high strength steels, Materialia 11 (2020) 100699.
[10] S.M. Lundberg, S.-I. Lee, A unified approach to interpreting model predictions, Proceedings of the 31st International Conference on Neural Information Processing Systems, Curran Associates Inc., Long Beach, California, USA, 2017, pp. 4768–4777.
[11] J.O. Ogutu, T. Schulz-Streeck, H.-P. Piepho, Genomic selection using regularized linear regression models: ridge regression, lasso, elastic net and their extensions, BMC Proceedings 6(2) (2012) S10.
[12] A.J. Smola, B. Schölkopf, A tutorial on support vector regression, Statistics and Computing 14(3) (2004) 199-222.
[13] L. Breiman, Random Forests, Machine Learning 45(1) (2001) 5-32.
[14] T. Chen, C. Guestrin, XGBoost: A Scalable Tree Boosting System, Proceedings of the 22nd ACM SIGKDD International Conference on Knowledge Discovery and Data Mining, Association for Computing Machinery, San Francisco, California, USA, 2016, pp. 785–794.
[15] B. Yegnanarayana, Artificial neural networks, PHI Learning Pvt. Ltd.2009.
[16] T. Akiba, S. Sano, T. Yanase, T. Ohta, M. Koyama, Optuna: A Next-generation Hyperparameter Optimization Framework, Proceedings of the 25th ACM SIGKDD International Conference on Knowledge Discovery & Data Mining, Association for Computing Machinery, Anchorage, AK, USA, 2019, pp. 2623–2631.
[17] A.E. Roth, The Shapley value: essays in honor of Lloyd S. Shapley, Cambridge University Press1988.